Giant enhancement of phonon-assisted one-photon excited frequency upconversion in a Nd3+-doped tellurite glass

M. S. Marques, L. de S. Menezes, W. Lozano B., L. R. P. Kassab, and C. B. de Araújo

Citation: Journal of Applied Physics **113**, 053102 (2013); doi: 10.1063/1.4789965
View online: http://dx.doi.org/10.1063/1.4789965
View Table of Contents: http://scitation.aip.org/content/aip/journal/jap/113/5?ver=pdfcov
Published by the AIP Publishing

Giant enhancement of phonon-assisted one-photon excited frequency upconversion in a Nd^{3+}-doped tellurite glass

M. S. Marques,[1,a)] L. de S. Menezes,[1,b)] W. Lozano B.,[1,c)] L. R. P. Kassab,[2] and C. B. de Araújo[1]
[1]*Departamento de Física, Universidade Federal de Pernambuco, Av. Prof. Luis Freire, s/n°, Cidade Universitária, Recife-PE 50670-901, Brazil*
[2]*Faculdade de Tecnologia de São Paulo, CEETEPS/UNESP, São Paulo-SP 01124-060, Brazil*

(Received 18 October 2012; accepted 15 January 2013; published online 1 February 2013)

Changing the sample's temperature from 200 K to 535 K, we observed 670-fold enhancement of a phonon-assisted upconversion emission at ≈754 nm obtained from a Nd^{3+}-doped tellurite glass excited by 5 ns laser pulses at 805 nm. A rate-equation model, including the relevant energy levels and temperature dependent transition rates, is proposed to describe the process. The results fit well with the data when one considers the nonradiative transitions contributing for the 754 nm luminescence are promoted by an effective phonon mode with energy of 700 cm^{-1}. © *2013 American Institute of Physics*. [http://dx.doi.org/10.1063/1.4789965]

I. INTRODUCTION

Frequency upconversion (UC) is a phenomenon in which light with wavelength smaller than the excitation wavelength is emitted by a physical system. This process finds many applications, such as infrared-pumped compact lasers in the visible range,[1] infrared-to-visible converters and light harvesting, important for solar cells,[2] temperature sensors,[3] and displays[4] among others.[5–8] Normally, UC is a nonlinear process, in which two or more photons from the excitation beam are used to generate one UC photon. The investigation of UC processes can be made studying the dependence of the photoluminescence (PL) intensity, I_S, versus the excitation laser intensity, I_L, given by $I_S \propto I_L^N$, where N is the number of laser photons for generation of each UC photon. Hence, normally one has $N \geq 2$ in a UC processes.

Changing the samples' temperature is an interesting possibility for controlling the UC spectrum exploiting phonon-assisted transitions in rare-earth (RE) doped materials. For example, this strategy was used in Ref. 9, in which an infrared-to-visible UC process was observed in Pr^{3+}/Yb^{3+} doped fluoroindate glass excited off-resonance with the RE transitions. More recently, UC emissions in $Yb^{3+}/Er^{3+}/Tm^{3+}$ and $Yb^{3+}/Ho^{3+}/Tm^{3+}$ co-doped lead-germanate glasses were obtained exciting the samples with an infrared laser.[10] The relative amount of red, green, and blue emissions in each sample depends on the relative concentration of the RE ions but it could be controlled as a function of the samples' temperature.

Due to the present interest in tellurite glasses (TG) for photonic applications, including those in which UC plays an important role, we performed experiments in TG samples doped with Nd^{3+} excited using a pulsed laser to investigate the temperature dependent UC process. TG are interesting materials for photonic applications, because they show a wide transmission window from 350 nm to 6.5 μm,[11] present low tendency for devitrification and small glass-transition temperature, having good chemical stability, high mechanical, and large thermal resistances, which are essential characteristics for, e.g., making optical fibers. Additionally, TG are attractive for devices, such as optical amplifiers and optical waveguides, since they present high refractive indices (≈2.0).[12] Besides this, they allow large RE doping levels[13] and present low cutoff-phonon energy (≈800 cm^{-1})[14] that are important characteristics for uses in luminescent devices.

This paper is organized as follows: Sec. II presents the fabrication procedure of Nd^{3+} doped TeO_2-ZnO (TZO) glasses and the main equipments used to characterize the samples. In Sec. III, we present details of the optical experiments performed to study the infrared-to-visible and infrared-to-infrared UC processes. The analysis of the experiments is mainly concentrated on the generation of UC luminescence at ≈ 754 nm (13, 262 cm^{-1}) due to the excitation of the samples with a laser operating in 805 nm (12, 422 cm^{-1}). The energy match in the process is due to the absorption of one incident laser photon followed by phonon annihilation. A rate-equation model is proposed to describe the results and a comparison between the present and previous works is made. Finally, in Sec. IV, we present a summary of the main results and conclusions.

II. EXPERIMENTAL DETAILS

The samples were prepared by the melt-quenching technique and had the composition (in mol. %) 85 TeO_2–13 ZnO–2 Nd_2O_3. Initially, the reagents are weighted, mixed, and homogenized in a platinum crucible. The mixture is introduced into an oven with no atmosphere control. After the mixture fusion, at 800 °C for 20 min, the liquid is cooled

[a)]Present address: Departamento de Ciêcias Humanas e Tecnologias, Universidade do Estado da Bahia, Campus XXIV, Xique-Xique-BA 47400-000, Brazil.
[b)]Author to whom correspondence should be addressed. Electronic mail: lmenezes@df.ufpe.br.
[c)]Permanent address: Facultad de Ciencias Físicas, Universidad Nacional Mayor de San Marcos–UNMSM, Lima, Perú.

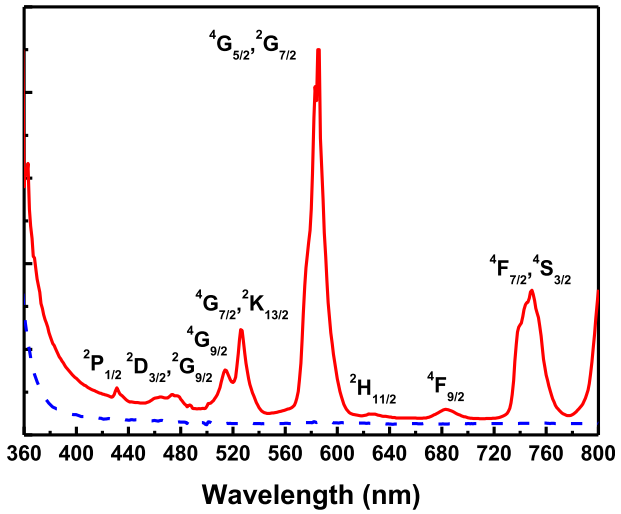

FIG. 1. Linear absorption spectrum of the Nd^{3+}- doped sample (red, solid line) and the undoped glassy matrix (blue, dashed line). The features are labeled with the excited levels when Nd^{3+} ions absorb light from the ground level $^4I_{9/2}$.

into a brass mold pre-heated to the annealing temperature (325 °C). Then, it is removed to another oven for completing the thermal treatment, at 325 °C during 2 h, for reduction of the internal stresses. After this, the oven is turned off and the sample is kept inside it until room temperature is reached. Afterwards, the glass is removed from the brass mold, cut, and polished.

The absorption spectra were obtained using a commercial spectrophotometer. The PL experiments were made using an optical parametric oscillator (400 kW, pulses of 5 ns, repetition rate: 20 Hz) operating at 805 nm, resonant with the $^4I_{9/2} \rightarrow {}^4F_{5/2}$ transition of the Nd^{3+} ions. The laser beam was focused on the sample by a 15 cm focal length lens; the PL was collected by a 5 cm focal length lens along a direction perpendicular to the laser propagation direction and sent to a spectrometer connected to a digital oscilloscope and a computer.

III. RESULTS AND DISCUSSION

Fig. 1 shows the absorption spectra of the Nd^{3+} doped sample and the undoped matrix. The absorption bands were identified by comparison with other Nd^{3+} -doped glass.[15] The spectrophotometer bandwidth was smaller than the absorption bands' linewidths, which are inhomogenously broadened.

The UC spectra can be seen in Figs. 2(a) and 2(b), where the bands' amplitudes are normalized by the largest band seen in each spectral range. The spectra show the Nd^{3+} PL lines (corresponding transitions) at 361 nm ($^4D_{3/2} \rightarrow {}^4I_{9/2}$), 386 nm ($^2P_{3/2} \rightarrow {}^4I_{9/2}$; $^4D_{3/2} \rightarrow {}^4I_{11/2}$), 417 nm ($^2P_{3/2} \rightarrow {}^4I_{11/2}$; $^4D_{3/2} \rightarrow {}^4I_{13/2}$), 431 nm ($^2D_{5/2}$,$^2P_{1/2} \rightarrow {}^4I_{11/2}$), 454 nm ($^4D_{3/2} \rightarrow {}^4I_{15/2}$), 486 nm ($^4G_{3/2} \rightarrow {}^4I_{9/2}$), 530 nm ($^4G_{7/2}$,$^2K_{13/2} \rightarrow {}^4I_{9/2}$; $^2K_{15/2} \rightarrow {}^4I_{11/2}$), 580 nm ($^2H_{11/2} \rightarrow {}^4I_{9/2}$), 595 nm ($^2G_{9/2} \rightarrow {}^4I_{13/2}$), 650 nm ($^4G_{7/2} \rightarrow {}^4I_{13/2}$), and 670 nm ($^2G_{9/2} \rightarrow {}^4I_{15/2}$). The PL intensities corresponding to these transitions show nonlinear dependences ($N \geq 2$) with the laser intensity[16] and their origin was already discussed by many authors in other glass matrices. In the present paper, we are interested only in the UC emission centered at 754 nm observed in Fig. 2(b) that corresponds to the $^4F_{7/2} \rightarrow {}^4I_{9/2}$ transition.

Although the PL signal centered at 754 nm is a UC emission, it presents a linear dependence ($N = 1$) with the excitation laser intensity, as shown in Fig. 3(a). Considering the excitation conditions and the intensity dependence of this UC emission, we concluded that this signal is originated in a process which starts with the resonant absorption $^4I_{9/2} \rightarrow {}^4F_{5/2}$ followed by annihilation of phonons that promote the excited ion to the thermally coupled $^4F_{7/2}$ level from where the PL at 754 nm originates. The UC pathway was verified measuring the temperature dependence of the PL intensity. Experimental data points are shown in Fig. 3(b) where a 670-fold PL enhancement is observed when the sample's temperature is changed from 200 K to 535 K, corresponding to a luminescence enhancement to temperature interval (LETI) = 670/335 K = 2.00/K.

The lines presented in Fig. 3(b), adjusted to the experimental data, represent the results of a model used to describe the UC pathway, illustrated in Fig. 4. In the model, the set of equations for the population densities (n_i; $i = 0, 1, 2, \alpha, \beta, \gamma$) of states $|0\rangle$ ($^4I_{9/2}$), $|1\rangle$ ($^4F_{5/2}$), $|2\rangle$ ($^4F_{7/2}$), $|\alpha\rangle$ ($^4F_{3/2}$), $|\beta\rangle$ ($^2P_{3/2}$), and $|\gamma\rangle$ ($^2P_{1/2}$) is

$$\begin{aligned}
\frac{dn_0}{dt} &= -W_{01}n_0 + \gamma_1 n_1 + \gamma_2 n_2 \\
\frac{dn_1}{dt} &= W_{01}n_0 - [W_{1\gamma}(T) + \Lambda_{12}(T) + \gamma_1 + W_1^{NR}(T)]\, n_1 \\
&\quad + W_{21}^{NR}(T) n_2 \\
\frac{dn_2}{dt} &= \Lambda_{12}(T)\, n_1 - [W_{2\beta}(T) + \gamma_2 + W_2^{NR}(T)]\, n_2. \qquad (1)
\end{aligned}$$

The measured signal at 754 nm is proportional to the maximum of the $n_2(t)$ function. The pump rate from the ground

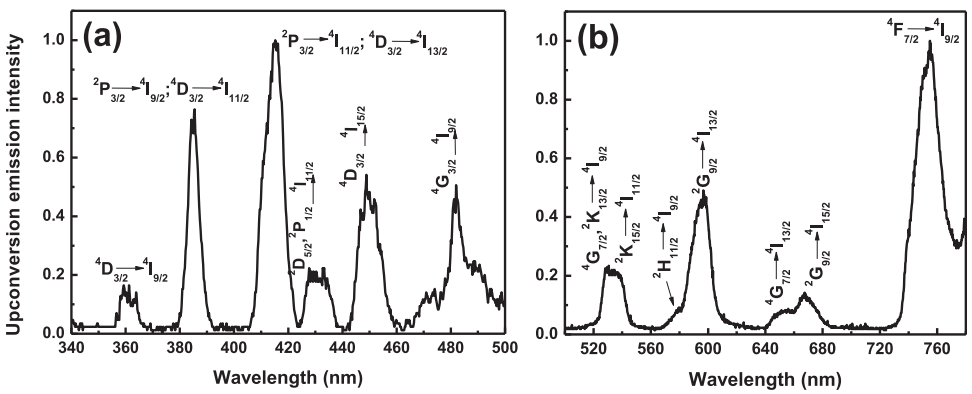

FIG. 2. Room temperature upconversion emission spectrum of Nd^{3+}- doped TZO for pulsed excitation at 805 nm.

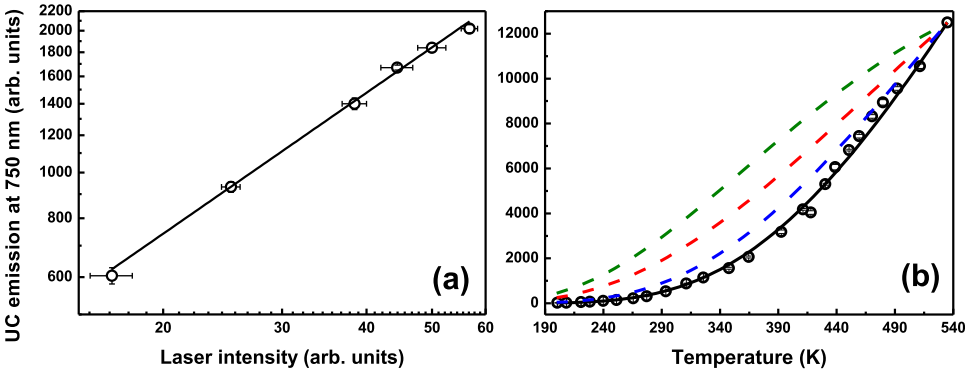

FIG. 3. (a) Dependence of the UC intensity at 754 nm versus the laser intensity at room temperature. The slope is $N = 1.0$, indicating that one laser photon is involved in the generation of each UC photon. (b) Comparison between the experimental data (circles) and the model results (lines). The curve which fits better the data is the one for an EPM of 700 cm^{-1} (black solid line). Also shown are the model results for some EPM energies (upper to lower dashed curves): 400 cm^{-1} (dashed green lines), 850 cm^{-1} (dashed red lines), and 600 cm^{-1} (dashed blue lines).

state W_{01} is $\sigma_{01}\Phi$, where σ_{01} is the (resonant) absorption cross section from the ground state $|0\rangle$ to the excited state $|1\rangle$, and Φ is the laser photon flux (the ratio between the laser intensity and the photon energy). The temperature-dependent pump rates $W_{ab}(T)$ are given by $\sigma_{ab}(T)\Phi$, where $\sigma_{ab}(T)$ ($ab = 1\gamma$ and 2β) are the temperature-dependent absorption cross-sections between levels a and b, being given by $\sigma_{ab}(T) = \sigma_{ab}^{RT}\left[\exp\left(\frac{h\nu}{kT} - 1\right)\right]^{-q_{ab}} = \sigma_{ab}^{RT}P_{ab}(T)$,[9] with σ_{ab}^{RT} being the absorption cross-section between levels a and b at room temperature; q_{ab} is the number of effective phonon modes (EPMs)[17] needed to bridge the gap between these two levels and $h\nu$ is the EPM energy. The population relaxation rate of level $i = 1,2$ is $\gamma_i = \gamma_i^{rad} + W_i^{NR}(T)$, with γ_i^{rad} being the radiative decay rate and $W_i^{NR}(T)$ is the temperature dependent nonradiative (NR) relaxation rate from level i to the next level below it due to multiphonon relaxation. According to Refs. 17 and 18, $W_i^{NR}(T)$ is given by $W_i^{NR}(T) = W_i^{NR}(T_0)\left[\frac{1-\exp(-h\nu/kT)}{1-\exp(-h\nu/kT_0)}\right]^{-p_i}$, where p_i is the number of EPMs needed to promote the NR transition from level i to its closest low-lying level. T_0 is the room temperature and $W_i^{NR}(T_0)$ is determined using the *energy-gap law*.[19] The multiphononic excitation rate is $\Lambda_{12}(T) = C_{12}^{e-p}P_{12}(T)$, with C_{12}^{e-p} being proportional to the electron-phonon coupling strength. The non-resonant absorption cross-sections were expressed as $\sigma_{ab}(\nu) = \sigma_{ab}^{0}\left[\exp\left(\frac{h\nu}{kT} - 1\right)\right]^{-q}$, where ν is the frequency detuning, σ_{ab}^{0} is the resonant cross-section between levels a and b, and q is the number of EPMs necessary for compensation of the energy mismatch. σ_{01} was obtained analyzing the oscillator strength ratios, R, between the transitions $|0\rangle \rightarrow |\alpha\rangle$ and $|0\rangle \rightarrow |1\rangle$ for different crystalline and glassy systems and multiplying this ratio by the absorption cross-section for the transition $|0\rangle \rightarrow |\alpha\rangle$.

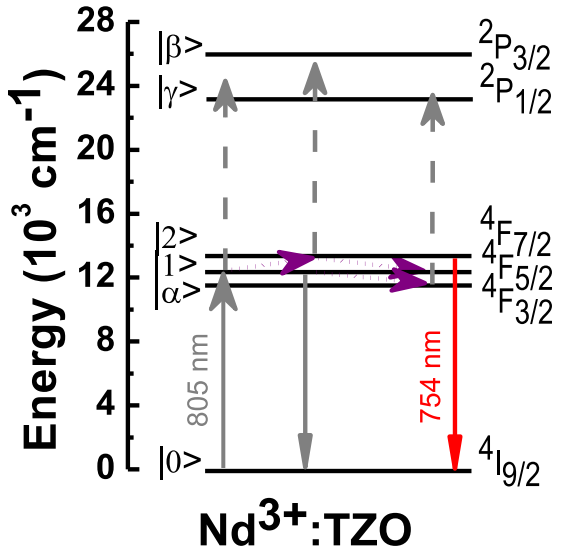

FIG. 4. Simplified energy levels scheme of Nd^{3+} representing the pathway to generate UC emission at 754 nm by exciting the sample at 805 nm. Solid (dashed lines) upward arrows represent laser excitation from the fundamental (excited) level. Dotted lines represent phonon-assisted temperature-dependent processes and the downward arrows represent radiative transitions.

According to Ref. 18, one has $\sigma_{0\alpha} = 5.0 \times 10^{-20}$ cm^2 and based on Ref. 20, one gets $R \approx 3.16$, leading to $\sigma_{01} = 1.5 \times 10^{-19}$ cm^2. For the other cross-sections, $\sigma_{1\gamma}$ and $\sigma_{2\beta}$, one sees from Ref. 21 that in crystals the typical values are in the range 10^{-22}–10^{-23} cm^2. Reference 19 presents results for other glasses that have the same order of magnitude. Thus, we considered the value 10^{-22} cm^2 for the resonant absorption cross-section of excited state transitions. Concerning the NR transition rates, from Ref. 19 one gets $W^{NR} \sim 10^9$ Hz for tellurite glasses at room temperature, for an energy gap of $\approx 10^3$ cm^{-1}, which is our case.

Other parameters included in the model are the radiative decay rates, γ_1 and γ_2. The value of γ_1, which is related to state $^4F_{5/2}$, was determined for various Nd^{3+} doped glasses; radiative lifetimes ranging from 750 μs[22] to 5 μs[23] were measured; on the other hand, data for γ_2 (related to the $^4F_{7/2}$ state) are less abundant.[23] However, our model is not much sensitive to these parameters, since the associated NR rates dominate in the range of temperatures studied here because the levels of interest are close-lying states. Thus, we considered $\gamma_1 = 10^5$ Hz and $\gamma_2 = 10^4$ Hz.

Then, solving the system of Eq. (1), varying the EPM energy and q_{ab}, q_i, and p, accordingly, we obtained the results shown in Fig. 3(b). The best fit to the experimental results corresponds to EPM energy of 700 cm^{-1}. For energies smaller than 700 cm^{-1}, the results deviate very much from the data, since a larger number of effective phonons are needed to bridge the relevant energy gaps, implying changes

in q_{ab}, q_i, and p that strongly influence the population dynamics. Deviation of the numerical results from the experimental data occurs also for EPM energies larger than 700 cm^{-1} as shown in Fig. 3(b).

From the basic point of view, the results of Fig. 3(b) indicate that it is not the matrix cutoff-phonon mode the one dominating the phonon-assisted UC transition, but the so-called EPM, which represents a statistical average that takes into account the phonon's energies and their occupation number.[17] From a more applied point of view, we recall that the observation of the phonon-assisted UC phenomenon in a fluoroindate glass[18] is very sensitive to the sample conditions including humidity and mechanical resistance of the fragile samples. In the TG case, the reproducibility of the results is less affected by the external conditions since TG in bulk and fibers forms are much more stable than fluoroindate glass. Another important point to consider is that because the UC process here reported requires only one EPM, it is more efficient than the previously reported cases that require participation of multiphonon transitions.

A comparison of the results with previous works allows a better evaluation of the present results. Resonant excitation of one-photon UC experiments in Nd^{3+} doped glasses involving annihilation of phonons was also exploited in two other systems. In Ref. 18, a Nd^{3+} doped fluoroindate glass was excited by a CW laser tuned to 866 nm, in resonance with the $^4I_{9/2} \rightarrow {}^4F_{3/2}$ transition of the Nd^{3+} ions. Many UC lines in the UV-VIS spectrum corresponding to $N \geq 2$ were detected as well as the UC emission at 750 nm that presented a linear ($N = 1$) intensity dependence versus the laser intensity. This process was explained as being due to one-photon absorption followed by multiphonon anhilation that supplied the energy necessary to promote the Nd^{3+} ions to the $^4F_{7/2}$ emitter state. The sample's temperature was varied from 298 K to 498 K, leading to 44-fold enhancement of the intensity at 750 nm, corresponding to a LETI = 0.22/K. More recently in Ref. 24, it was reported an experiment with a Nd^{3+} doped $LiTeO_2$ glass excited with a CW laser at 800 nm. UC luminescence at 755 nm was detected but its power dependence was not reported. Its intensity dependence on the samples' temperature was recorded; the results show a 90-fold enhancement within the range 298 K to 523 K, meaning a LETI = 0.40/K. Both LETI results of Refs. 18 and 24 are smaller than in the present case.

IV. CONCLUSIONS

We studied a thermally activated UC emission in a Nd^{3+}-doped tellurite glass by resonant excitation of transition $^4I_{9/2} \rightarrow {}^4F_{5/2}$ at 805 nm. The UC emission at 754 nm due to transition $^4F_{7/2} \rightarrow {}^4I_{9/2}$ presented linear intensity dependence versus the laser intensity and experienced 670-fold enhancement when the sample's temperature changes from 200 K to 535 K, the largest in the best of the authors' knowledge for thermally assisted one-photon induced UC emission. A model considering the relevant energy levels populations, including temperature-dependent absorption cross-sections and nonradiative transition rates, was proposed to describe the thermal behavior of the UC process. The temperature dependence of the one-photon excited UC emission is well described considering an EPM with energy of 700 cm^{-1}.

ACKNOWLEDGMENTS

This work was supported by the Conselho Nacional de Desenvolvimento Científico e Tecnológico (CNPq), through the INCT de Fotônica project and by a joint grant from CNPq and FACEPE (Fundação de Amparo à Ciência e Tecnologia do Estado de Pernambuco) through the PRONEX program. The authors are grateful to Dr. Kelly C. Jorge for helping with the Mathcad® code.

[1]R. Scheps, Prog. Quantum Electron. **20**, 271 (1996).
[2]H.-Q. Wang, M. Batentschuk, A. Osvet, L. Pinna, and C. J. Brabec, Adv. Mater. **23**, 2675 (2011).
[3]G. S. Maciel, L. de S. Menezes, A. S. L. Gomes, C. B. de Araújo, Y. Messaddeq, A. Florez, and M. A. Aegerter, IEEE Photon. Technol. Lett. **7**, 1474 (1995).
[4]E. Downing, L. Hesselink, J. Ralston, and R. Macfarlane, Science **273**, 1185 (1996).
[5]F. Wang and X. G. Liu, Chem. Soc. Rev. **38**, 976 (2009).
[6]C. B. de Araújo, G. S. Maciel, L. de S. Menezes, N. Rakov, E. L. Falcão-Filho, V. A. Jerez, and Y. Messaddeq, C. R. Chim. **5**, 885 (2002).
[7]F. Auzel, Chem. Rev. **104**, 139 (2004).
[8]D. R. Gamelin and H. U. Güdel, Acc. Chem. Res. **33**, 235 (2000).
[9]A. S. Oliveira, E. A. Gouveia, M. T. de Araújo, A. S. Gouveia-Neto, C. B. de Araújo, and Y. Messaddeq, J. Appl. Phys. **87**, 4274 (2000).
[10]A. S. Gouveia-Neto, L. A. Bueno, R. F. Nascimento, E. A. Silva, and E. B. da Costa, Mater. Lett. **63**, 1999 (2009).
[11]K. U. Kumar, V. Prathyusha, P. Babu, C. Jayasankar, A. Joshi, A. Speghini, and M. Bettinelli, Spectrochim. Acta A **67**, 702 (2007).
[12]J. Wang, E. Vogel, and E. Snitzer, Opt. Mater. **3**, 187 (1994).
[13]R. A. H. El-Mallawany, *Tellurite Glass Handbook: Physical Properties and Data* (CRC, Boca Raton, 2001).
[14]L. R. P. Kassab, R. A. Kobayashi, M. J. V. Bell, A. P. Carmo, and T. Catunda, J. Phys. D: Appl. Phys. **40**, 4073 (2007).
[15]C. X. Cardoso, Y. Messaddeq, L. A. O. Nunes, and M. A. Aegerter, J. Non-Cryst. Solids **161**, 277 (1993).
[16]M. S. Marques, "Frequency upconversion and thermal effects in phonon-assisted transitions in Nd^{3+} doped tellurite glasses," M.S. thesis (Universidade Federal de Pernambuco, 2011) (in Portuguese).
[17]F. Auzel, Phys. Rev. B **13**, 2809 (1976).
[18]L. de S. Menezes, G. S. Maciel, C. B. de Araújo, and Y. Messaddeq, J. Appl. Phys. **90**, 4498 (2001).
[19]M. Yamane and Y. Asahara, *Glasses for Photonics* (Cambridge University Press, Cambridge, UK, 2000).
[20]W. F. Krupke, Phys. Rev. **145**, 325 (1966).
[21]R. Reisfeld and C. Jorgensen, *Lasers and Excited States of Rare-Earths* (Springer-Verlag, Berlin, 1977), p. 103.
[22]G. Poza, D. Ajò, M. Bettinelli, A. Speghini, and M. Casarin, Solid State Commun. **97**, 521 (1996).
[23]L. de S. Menezes, "Energy upconversion in Nd^{3+} doped fluoroindate glasses," M.S. thesis (Universidade Federal de Pernambuco, 1996) (in Portuguese).
[24]K. Kumar, S. B. Rai, and D. K. Rai, Eur. Phys. J.: Appl. Phys. **41**, 143 (2008).